Spectroscopic States of the CO Oxidation/CO_2 Reduction Active Site of Carbon Monoxide Dehydrogenase and Mechanistic Implications†

Mark E. Anderson‡ and Paul A. Lindahl*

Department of Chemistry, Texas A&M University, College Station, Texas 77843

Received December 8, 1995; Revised Manuscript Received February 26, 1996⊗

ABSTRACT: CO dehydrogenases catalyze the reversible oxidation of CO to CO_2, at an active site (called the C-cluster) composed of an Fe_4S_4 cube with what appears to be a 5-coordinate Fe (called FCII), linked to a Ni (Hu, Z., Spangler, N. J., Anderson, M. E., Xia, J., Ludden, P. W., Lindahl, P. A., & Münck, E. (1996) *J. Am. Chem. Soc. 118*, 830−845). During catalysis, electrons are transferred from the C-cluster to an $[Fe_4S_4]^{2+/1+}$ electron-transfer cluster called the B-cluster. An $S = {}^1/_2$ form of the C-cluster (called C_{red1}) converts to another $S = {}^1/_2$ form (called C_{red2}) upon reduction with CO, at a rate well within the turnover frequency of the enzyme (Kumar, M., Lu, W.-P., Liu, L., & Ragsdale, S. W. (1993) *J. Am. Chem. Soc. 115*, 11646−11647). This suggests that the conversion is part of the catalytic mechanism. Dithionite is reported in this paper to effect this conversion as well, but at a much slower rate ($k_{so} = 5.3 \times 10^{-2}$ M^{-1} s^{-1} for dithionite *vs* 4.4×10^6 M^{-1} s^{-1} for CO). By contrast, dithionite reduces the oxidized B-cluster much faster, possibly within the turnover frequency of the enzyme. Dithionite apparently effects the C_{red1}/C_{red2} conversion directly, rather than through an intermediate. The conversion rate varies with dithionite concentration. The C_{red1}/C_{red2} conversion occurs at least 10^2 times faster in the presence of CO_2 than in its absence. CO_2 alters the *g* values of the $g_{av} = 1.82$ signal, indicating that CO_2 binds to a C-cluster-sensitive site at mild potentials. CN^- inhibits CO oxidation by binding to FCII (Hu et al., 1996), and CO, CO_2 in the presence of dithionite, or CS_2 in dithionite accelerate CN^- dissociation from this site (Anderson, M. E., & Lindahl, P. A. (1994) *Biochemistry 33*, 8702−8711). The effect of CO, CO_2, and CS_2 on CN^- dissociation suggested that these molecules bind at a site (called the modulator) other than that to which CN^- binds. The effects of CO_2, CS_2, CO, and dithionite on the C_{red1}/C_{red2} conversion rate followed a similar pattern, suggesting that this rate is also influenced by modulator binding. Some batches of enzyme cannot convert to the C_{red2} form using dithionite, but pretreatment with CO or CO_2/dithionite effectively "cures" such batches of this disability. The results presented suggest that the Ni of the C-cluster is the modulator and the substrate binding site for CO/CO_2. The inhibitor CS_2 in the presence of dithionite also accelerates the decline of C_{red1}, leading first to an EPR-silent state of the C-cluster, and eventually to a state yielding an EPR signal with $g_{av} = 1.66$. CS_2 binding thus shares some resemblance to CO_2 binding. Approximately 90% of the absorbance changes at 420 nm that occur when oxidized $CODH_{Ct}$ is reduced by dithionite occur within 2 min at 10 °C. This absorbance change occurs in concert with the $g_{av} = 1.94$ signal development. The remaining 10% of the A_{420} changes occur over the course of ∼50 min, apparently coincident with the C_{red1}/C_{red2} conversion. One possibility is that the conversion involves reduction of an (unidentified) Fe-S cluster. A three-state model of catalysis is proposed in which C_{red1} binds and oxidizes CO, C_{red2} is two electrons more reduced than C_{red1} and is the state that binds and reduces CO_2, and C_{int} is a one-electron-reduced state that is proposed to exist because of constraints imposed by the nature of the CO/CO_2 reaction and the properties of the clusters involved in catalysis.

Carbon monoxide dehydrogenases (CODH)[1] are one of only four known types of naturally occurring Ni containing enzymes. They are found in certain acetogenic, methanogenic, and photosynthetic bacteria, where they catalyze the reversible oxidation of CO to CO_2. CODH's from acetogenic bacteria also participate in the synthesis of acetyl-CoA (the Wood/Ljungdahl pathway), and methanogenic CODH's additionally participate in the synthesis of methane from acetyl-CoA (acetoclastic methanogenesis) (Wood & Ljungdahl, 1991; Ragsdale, 1991; Roberts et al., 1992).

Carbon monoxide dehydrogenase from the acetogen *Clostridium thermoaceticum* ($CODH_{Ct}$) has an $\alpha_2\beta_2$ tetrameric quaternary protein structure (Xia et al., 1996). The α and β subunits have masses of 81 730 and 72 928 Da, respectively (Morton et al., 1991). Each $\alpha\beta$ dimer contains 2 Ni, 11−13 Fe, and ∼14 S^{2-} ions (Ragsdale et al., 1983; Lindahl et al., 1990a). These metal ions are arranged into three types of clusters, called the *A-, B-, and C-clusters*.[2] The A-cluster is the active site for acetyl-CoA synthesis (Gorst & Ragsdale, 1991; Shin & Lindahl, 1992a,b; Shin et al., 1993). It appears to consist of a Ni center exchange-coupled to an Fe_4S_4 cluster (Ragsdale et al., 1985; Lindahl et al., 1990b; Fan et al., 1991; Xia & Lindahl, 1996) and is

† This research was supported by the National Institutes of Health (GM46441) and the Robert A. Welch Foundation (A1170).

* To whom correspondence should be addressed.

‡ Present address: Department of Biochemistry and Molecular Biology, University of South Florida College of Medicine, 12901 Bruce B. Downs Blvd., Tampa, FL 33612.

⊗ Abstract published in *Advance ACS Abstracts,* June 1, 1996.

S0006-2960(95)02902-3 CCC: $12.00 © 1996 American Chemical Society

located in the α subunit. The A-cluster is stable in a diamagnetic oxidized state (A_{ox}) and a one-electron-reduced state with CO bound (A_{red}-CO) (Lindahl et al., 1990b; Kumar & Ragsdale, 1992; Qiu et al., 1994, 1995). This reduced state exhibits the so-called NiFeC EPR signal (Ragsdale et al., 1982, 1983, 1985). A_{red}-CO appears to be the catalytically active state of the A-cluster (Lu & Ragsdale, 1991).

The C-cluster is the active site for CO oxidation and CO_2 reduction (Kumar et al., 1993; Anderson et al., 1993; Anderson & Lindahl, 1994) and is apparently located in the β subunit (Xia & Lindahl, 1995; Xia et al., 1996). It is diamagnetic when oxidized, and $S = {}^1/_2$ when reduced by one electron ($E^{\circ\prime} = -220$ mV *vs* NHE; Lindahl et al., 1990a). The reduced state exhibits an EPR signal with $g_{av} = 1.82$ (the C_{red1} state). As potentials are lowered ($E_m = -530$ mV), the $g_{av} = 1.82$ signal disappears and is replaced by another signal with $g_{av} = 1.86$ (the C_{red2} state; Lindahl et al., 1990a). Hu et al. (1996) recently used Mössbauer spectroscopy to determine that the C-cluster is an Fe_4S_4 cluster with what appears to be a 5-coordinate Fe (labeled FCII) that is probably bridged to a Ni ion. In the C_{red1} state, the cluster is in the 1+ core oxidation state, and the Ni appears to be in the 2+ state. The Ni may or may not participate in the spin-coupling arrangement yielding the $g_{av} = 1.82$ state.

The C_{red1}/C_{red2} conversion is not well understood, but it appears to be involved in catalysis. Kumar et al. (1993) found that this conversion is the first EPR-detectable event to occur when partially-oxidized $CODH_{Ct}$ is reduced with CO. It occurs well within the turnover frequency of the enzyme ($k_{conversion} = 400\ s^{-1}$ compared to $k_{cat} = 47\ s^{-1}$ at 5 °C), and at a rate that depends on CO concentration. We previously proposed, and now summarize in eq 1, that CO binds to and is oxidized by C_{red1}, that CO_2 binds to and is reduced by C_{red2}, and that C_{red2} is two electrons more reduced than C_{red1} (Anderson & Lindahl, 1994):

$$[C_{red2}]^{(n-2)+} + CO_2 + H^+ \rightleftharpoons [C_{red1}]^{(n+)} + CO + OH^- \quad (1)$$

We proposed this because the midpoint potential for the conversion is near to the reduction potential for CO/CO_2 (as expected for reversible catalysis), and the two states are separated by an even number of electrons (as required by the $n = 2$ nature of the CO/CO_2 redox process). Alternatively, C_{red2} and C_{red1} may be isoelectronic and the conversion may reflect a redox-dependent conformational change triggered when some unidentified species (designated Y in footnote 6) besides the C-cluster is reduced (in which case $E^{\circ\prime}$ for Y_{ox}/Y_{red} would be −530 mV). A third possibility, that C_{red2} is an isoelectronic CO-bound form of C_{red1}, can be ruled out since dithionite and other low-potential nonligating reductants (e.g., viologens) can also effect this conversion and afford the C_{red2} state.

The mechanism of CO oxidation is thought to involve the binding and deprotonation of water at a metal site of the C-cluster (Seravalli et al., 1995). CO is thought to bind to an adjacent site of the C-cluster, followed by attack of a metal-bound hydroxide on the carbonyl carbon, forming a metal-bound carboxylate. After deprotonation, CO_2 is thought to leave, affording a two-electron-reduced form of the C-cluster. Electrons are then transferred from the C-cluster through the B-cluster (an $[Fe_4S_4]^{2+/1+}$ cluster) to external electron acceptors (Kumar et al., 1993; Anderson & Lindahl, 1994).

Cyanide is a potent inhibitor of the CO oxidation reaction. Hu et al. (1996) found that CN^- binds to the novel FCII iron of the C-cluster in the C_{red1} form. Binding shifts the $g_{av} = 1.82$ signal to one with $g_{av} = 1.72$ (Anderson et al., 1993). CN^- is a slow-tight-binding inhibitor that does not readily dissociate, even after removing free CN^- and diluting CN^--inhibited samples 100-fold (Anderson & Lindahl, 1994). CN^- does dissociate over the course of ∼1 h at room temperature if samples are exposed to CO, CO_2 in the presence of dithionite (CO_2/dithionite), or CS_2/dithionite. Dithionite by itself is ineffective in CN^- dissociation. Anderson and Lindahl (1994) concluded that CO, CO_2, and CS_2 bind at a site, called the *modulator*, other than that to which CN^- binds (presumed at that time to be the active site). According to this view, CN^- and either CO, CO_2, or CS_2 are not competing for the same site and can bind simultaneously to the enzyme.

The modulator has not been spectroscopically identified, and further evidence is required to establish its existence. We postulated such a site so that the following properties of the enzyme could be explained. First, CN^- that is bound to $CODH_{Ct}$ does not dissociate when the enzyme is separated from any unbound CN^- and diluted 100-fold. If CO and CN^- competed for the same site on the enzyme, the rate of CN^- dissociation under these circumstances would be similar to the rapid dissociation rate obtained by exposing CN^--inhibited samples to CO. Second, competitive binding requires that CO binds the C_{red2} state of the C-cluster (to explain how CO protects $CODH_{Ct}$ in this state against CN^- inhibition), but the C_{red2} state could be attained by adding dithionite or reduced viologens in the absence of CO. Finally, CS_2/dithionite causes the dissociation of CN^- from the C-cluster although CS_2 was reported to be a weak *noncompetitive* inhibitor of CO oxidation.

[1] Abbreviations: CODH, carbon monoxide dehydrogenase; $CODH_{Ct}$, CODH from *Clostridium thermoaceticum*; $CODH_{Rr}$, CODH from *Rhodospirillum rubrum*; EPR, electron paramagnetic resonance; A_{ox}, the diamagnetic oxidized A-cluster state; A_{red}-CO, the A-cluster state exhibiting the NiFeC EPR signal, obtained when $CODH_{Ct}$ is reduced and bound with CO; B_{ox}, the diamagnetic oxidized B-cluster state; B_{red}, the reduced B-cluster state, exhibiting the $g_{av} = 1.94$ signal; C_{ox}, the diamagnetic state of the C-cluster; C_{red1}, the C-cluster state exhibiting the $g_{av} = 1.82$ signal in $CODH_{Ct}$; C_{red2}, the C-cluster state exhibiting the $g_{av} = 1.86$ signal in $CODH_{Ct}$; C_{int}, a proposed C-cluster state one electron more reduced than C_{red1} and one electron more oxidized than C_{red2}; C_{sum}, the sum of the $g_{av} = 1.82$ and $g_{av} = 1.86$ EPR signal intensities; Y_{ox}/Y_{red}, the oxidized and reduced form of the proposed EPR-silent redox-active species required by the isoelectronic model to cause the C_{red1}/C_{red2} conversion; C_{red12}, the C-cluster state of the isoelectronic model which exhibits the $g_{av} = 1.82$ and $g_{av} = 1.86$ signals in $CODH_{Ct}$ as determined by the redox status of species Y; $C_{superred}$, a proposed state of the C-cluster two electrons more reduced than C_{red12}; X_{ox}/X_{red}, the oxidized and reduced forms of the proposed $n = 1$ EPR-silent redox-active species that is reduced by C_{int} and oxidized by C_{red1}; L_{ox}/L_{red}, the oxidized and reduced forms of the proposed $n = 1$ redox-active ligand to the Ni in the C-cluster; FCII, the Fe in the Fe_4S_4 component of the C-cluster that appears to be 5-coordinate; k_{so}, the second-order rate constant for the dithionite-induced C_{red1}/C_{red2} conversion; k_{obs}, the observed apparent first-order rate constant for the C_{red1}/C_{red2} conversion; NHE, normal hydrogen electrode.

[2] The A-, B-, and C-clusters were previously called the *NiFe Complex*, the *FCI-associated Fe_4S_4 Cluster*, and the *$g_{av} = 1.82$ Species*, respectively. Anderson and Lindahl (1994) referred to C_{red1} and C_{red2} as C_{182} and C_{186}, respectively. Kumar et al. (1993) referred to the same states as *C* and *C′*, respectively.

Another unusual property of $CODH_{Ct}$ is that A_{ox} can only be reduced in a limited number of ways. It can be reduced with CO, but not by low-potential viologens or dithionite (Lindahl et al., 1990a,b). Curiously, A_{ox} *can* be reduced by viologens or dithionite in the presence of CO, CO_2, or CS_2 (Anderson & Lindahl, 1994). With CS_2, reduction of A_{ox} affords an EPR signal with $g_{av} = 2.15$ rather than the NiFeC signal (Kumar et al., 1994). Evidence that dithionite can reduce A_{ox} in the presence of CO was difficult to obtain, since CO itself can reduce A_{ox}. Anderson and Lindahl (1994) found that incubation of CN^--inhibited $CODH_{Ct}$ in dithionite and CO afforded the NiFeC signal (indicative of A_{red}-CO) at a rate that was *faster* than CN^- dissociated from the C-cluster (Figure 10, Anderson & Lindahl, 1994). With CN^- bound at the C-cluster, CO could not reduce the clusters in the enzyme (Figure 7, Anderson & Lindahl, 1994), leaving dithionite as the only possible reductant of A_{ox}. Why can dithionite reduce A_{ox} in the presence of CO, CO_2, and CS_2 but not in their absence? Since this "reactivity pattern" was similar to that observed for the dissociation of CN^- (namely, that CO, CO_2/dithionite, or CS_2/dithionite could effect a phenomenon that dithionite alone could not effect), Anderson and Lindahl (1994) suggested that the reduction of A_{ox} was controlled by modulator binding; i.e., that electrons can be delivered to A_{ox} either from the C-cluster, from the B-cluster, or from dithionite as long as CO, CO_2, or CS_2 was bound to the modulator.

In this paper, we report the first spectroscopic evidence for a modulator site (a CO_2-dependent shift of the $g_{av} = 1.82$ EPR signal), describe another apparent affect of modulator binding (a CO_2-dependent C_{red1}/C_{red2} conversion rate), and provide some evidence that modulator binding induces a protein conformational change. We also probe the difference between the C_{red1} and C_{red2} states by electronic absorption spectroscopy, and characterize the effects of CO_2 and CS_2 on the enzyme. Arguments are made that the Ni component of the C-cluster is the modulator, that the C-cluster traverses three sequential redox states during catalysis, and that the Ni has a 1+ valence in the C_{red2} state.

EXPERIMENTAL PROCEDURES

Cultures of *C. thermoaceticum* were grown, and two batches of $CODH_{Ct}$ were purified and characterized as described (Lundie & Drake, 1984; Shin & Lindahl, 1993). Batches 1 and 2 were >90% pure according to SDS−PAGE (Weber & Osborn, 1969) and had 410 and 490 units/mg CO oxidation activity, and 0.1 and 0.3 unit/mg CO/acetyl-CoA exchange activity, respectively. $CODH_{Ct}$ samples were buffered in 50 mM Tris, pH 8. All procedures involving $CODH_{Ct}$ were performed either in an argon-atmosphere glovebox (Vacuum/Atmospheres HE453) containing 0.5−1 ppm oxygen as monitored continuously (Teledyne Model 310 oxygen analyzer) or on CO or CO_2 Schlenk manifolds. EPR spectra were recorded and quantified as described (Shin et al., 1992), using a 1.0 mM copper perchlorate standard. Protein concentrations were determined by the biuret method (Pelley et al., 1978). CS_2 (Fisher) was purified as described (Gordon & Ford, 1971), and analyzed by GCMS (HP Model 5970A detector; 5890 GC; 59970A workstation; 50 m × 0.2 mm i.d. cross-linked methylsilcone column; elution temperature, 80 °C) and HPLC (Waters, Model 600, 3.9 × 150 mm C_{18} column, 25 °C in methanol), and was found to be 99% pure. Sodium dithionite (Aldrich) was standardized against potassium ferricyanide. Thionin (3,7-diaminophenothiazin-5-ium chloride, Aldrich) was standardized against the dithionite. Both dithionite and thionin were standardized immediately before experiments.

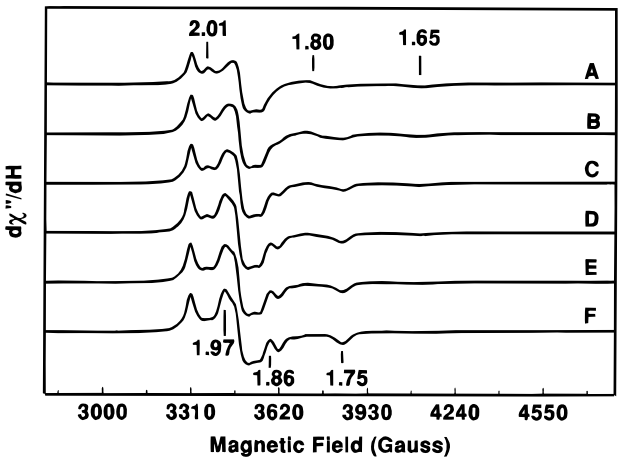

FIGURE 1: Kinetics of the dithionite-induced C_{red1}-to-C_{red2} conversion at 1 °C. $CODH_{Ct}$ (32 μM $\alpha\beta$, batch 1) was cooled to 1 °C, and then oxidized with a slight excess of thionin. The conversion reaction was initiated by adding dithionite (0.11 mM final concentration). Aliquots were withdrawn periodically and quickly frozen in a LN_2-cooled isopentane bath at the following times: (A) 1.4 min; (B) 74 min; (C) 150 min; (D) 230 min; (E) 300 min; (F) 600 min. Similar experiments were performed using the same batch of $CODH_{Ct}$ and 0.98, 2.8, and 3.8 mM dithionite. EPR conditions for all figures: microwave frequency, 9.43−9.44 GHz; microwave power, 20 mW; temp, 10 K; time constant, 328 ms; modulation amplitude, 11 G; modulation frequency, 100 kHz.

For the optical study, a 10/30 outer ground-glass joint and a double-septum-sealed port (Averill & Orme-Johnson, 1978) were attached to a 1-cm path length quartz optical cuvette (Starna, 1-Q-10/GS). A thermocouple was sealed with epoxy through an inner 10/30 ground-glass joint, and this joint was sealed into the outer joint of the cuvette. UV−vis spectra were obtained on a Hewlett Packard 8452A diode-array spectrophotometer with 89531A software. The antifreeze-cooled sample-holder was attached to a Haake A81 constant-temperature circulating bath.

To render batch 1 of $CODH_{Ct}$ able to be converted fully to the C_{red2} state by dithionite, samples were freed of dithionite and salts using a Sephadex G25 column equilibrated in 50 mM Tris, pH 8, exposed to 1 atm CO for ∼3 min, allowed to degas under Ar for ∼1 h, and then oxidized with a slight excess of thionin. The dithionite kinetic experiments were performed on such CO-treated $CODH_{Ct}$.

RESULTS

Rate of Dithionite-Induced C_{red1}/C_{red2} Conversion. When thionin-oxidized $CODH_{Ct}$ was reduced by dithionite, the rate of conversion from C_{red1} to C_{red2} was slow enough to be followed by manual mixing and slow freezing methods. At 1 °C and using 0.11 mM dithionite, C_{red1} converted to C_{red2} in ∼10 h (Figure 1). Similar experiments were performed using 0.98, 2.8, and 3.8 mM dithionite.[3] The simplest model explaining this conversion assumes that C_{red2} is two electrons more reduced than C_{red1} and that dithionite reduces C_{red1} directly to C_{red2}, according to the following equation:

$$[C_{red1}]^{n+} \xrightarrow{k_{obs} = k_{so}[S_2O_4^{2-}]} [C_{red2}]^{(n-2)+} \qquad (2)$$

This model requires that the sum of the $g_{av} = 1.82$ and 1.86 signal intensities be invariant with time. To check this, these intensities were quantified and summed for each point of the reaction. The summed intensities were invariant within the scatter of the data (±20%), and thus support this model.[4]

The model also requires that the rate of C_{red1} decay equals the rate of C_{red2} development. To check this, these rates were analyzed independently using the following equations:

$$[C_{red1}]_t = [C_{sum}]e^{-kt} \quad (3)$$

$$[C_{red2}]_t = [C_{sum}](1 - e^{-kt}) \quad (4)$$

C_{sum} is the summed $g_{av} = 1.82 + 1.86$ signal intensities, averaged over all data points. Plots of $\ln([C_{red1}]_t/[C_{sum}])$ *vs* time (circles) and $\ln(1 - ([C_{red2}]_t/[C_{sum}]))$ *vs* time (triangles), along with the corresponding least-squares best fits to the data (solid and dotted lines, respectively) are shown in Figure 2. The apparent first-order rate constants for both decay and development reactions are given in Table 1. For the experiments using 0.11, 2.8, and 3.8 mM dithionite, the best-fit values of k obtained for C_{red1} decay deviated from those for the corresponding C_{red2} development by only 10%. This is further support for the model. The corresponding rate constants for the 0.98 mM experiment differed somewhat more (by 28%), not enough to be inconsistent with the model.

These rates (ranging from 4.7×10^{-5} s^{-1} to 38×10^{-5} s^{-1}) are orders of magnitude slower than k_{cat} for CO oxidation at this temperature (47 s^{-1}). Nevertheless, it would be incorrect to conclude that this conversion is catalytically irrelevant, since it occurs substantially faster than k_{cat} ($k_{conversion} = 400$ s^{-1}) when the substrate CO is the reductant (Kumar et al., 1993). We do not understand why the conversion is slower with dithionite, but it allowed the conversion to be studied in more detail.

As required by eq 2, the best-fit first-order apparent rate constants increased with dithionite concentration. Analysis using the relationship $k = k_{so}[S_2O_4^{2-}]$ yielded the second-order rate constant $k_{so} = 5.3 \times 10^{-3}$ M^{-1} s^{-1}. The observed trend in rates suggests that dithionite reduces the site responsible for the C_{red1}/C_{red2} conversion (assumed here to be C_{red1} itself), at or before the rate-limiting step in the conversion process. The number and range of data points are insufficient to exclude the possibility that the trend in rates actually depends on the $SO_2^{\bullet-}$ concentration rather than on $S_2O_4^{2-}$. In this case, the C-cluster would be reduced to C_{red2} via an EPR-silent one-electron-reduced form called C_{int}, as shown:

$$[C_{red1}]^{n+} \xrightarrow{k_1[SO_2^-]} [C_{int}]^{(n-1)+} \xrightarrow{k_2[SO_2^-]} [C_{red2}]^{(n-2)+} \quad (5)$$

The data require that $k_1 < k_2$, for otherwise the intensity of C_{int} would build up and the decay rate of C_{red1} would not equal the development rate of C_{red2}.

Dithionite Reduction of B_{ox}. The rate at which dithionite reduced B_{ox} was substantially faster than the C_{red1}/C_{red2} conversion rate. We quantified the $g_{av} = 1.94$ signal at each point of the four experiments and plotted the normalized values *vs* time (data not shown).[4] The B-cluster was >90% reduced within the time of manual mixing and freezing (~10 s). Thus, dithionite does not appear to reduce the B-cluster exclusively via the C_{red2} form of the C-cluster. It may reduce B_{ox} directly. The rapid reduction of B_{ox} supports the proposed electron-transfer role of the B-cluster in catalysis.

Effect of CO_2 on C_{red1}. A sample of thionin-oxidized $CODH_{Ct}$ was exposed to CO_2 and then frozen. It exhibited an EPR signal from the C-cluster (Figure 3B) with $g_{av} = 1.85$ ($g = 2.01, 1.84, 1.68$). The control sample prepared in the absence of CO_2 exhibited a typical $g_{av} = 1.82$ signal ($g = 2.01, 1.80, 1.65$; Figure 3A). The shift in g values in the presence of CO_2 indicates that CO_2 is binding to the

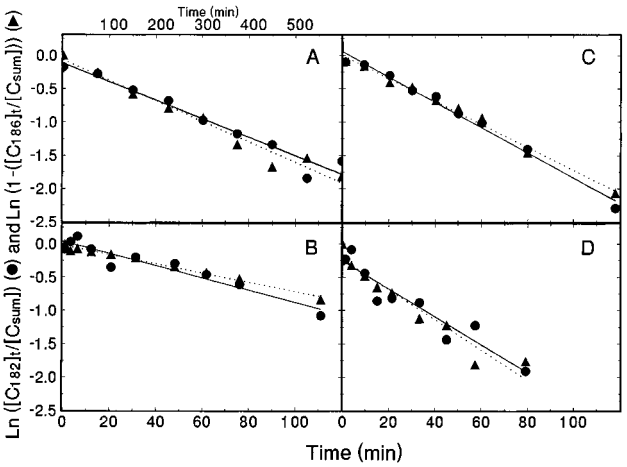

FIGURE 2: Analysis of $g_{av} = 1.82$ decay and $g_{av} = 1.86$ development kinetics. The $g_{av} = 1.82$ and 1.86 signal intensities from the experiments of Figure 1 were analyzed using eqs 3 and 4, respectively. For each experiment, $g_{av} = 1.82$ and 1.86 intensities at each data point were summed, and the summed values were averaged. The $g_{av} = 1.82$ signal intensities were then divided by this averaged value, and the natural log of these ratios were plotted (circles) *vs* time after adding dithionite to thionin-oxidized $CODH_{Ct}$. The $g_{av} = 1.86$ signals were divided by the same averaged value, subtracted from 1, and plotted similarly (triangles). The lines are the least-squares best fits to the data, with slopes equal to the negative apparent first-order rate constants, $-k$ (values given in Table 1). (A) 0.11 mM dithionite. The time parameter for this experiment is given at the top of the plot. (B) 0.98 mM dithionite. (C) 2.8 mM dithionite. (D) 3.8 mM dithionite. The times for these experiments are given at the bottom of the plots.

Table 1: Apparent First-Order Rate Constants for C_{red1} Decay and C_{red2} Development

[dithionite] (mM)	C_{red1} decay $k \times 10^{-3}$ (min^{-1})	C_{red2} development $k \times 10^{-3}$ (min^{-1})
0.11	2.8	3.1
0.98	9.2	7.0
2.8	19	17
3.8	21	23

[3] Similar experiments were also performed using 5.8, 6.5, and 9.4 mM dithionite, but scatter in the data precluded reliable analysis. The C_{red1}/C_{red2} conversion rates did increase in proportion to the dithionite concentration in these experiments, except for that using 9.4 mM dithionite, which yielded an anomolously low rate. Factors such as sample history may have affected the rate observed.

[4] The sum of the $g_{av} = [1.82 + 1.86]$ signal intensities for the samples reduced with 0.11 mM dithionite (obtained from the spectra of Figure 1) varied from 0.21 to 0.28 spin/$\alpha\beta$. Similar intensities for the samples reduced with 0.98, 2.8, and 3.8 mM dithionite were 0.24−0.26 spin/$\alpha\beta$, 0.20−0.28 spin/$\alpha\beta$, and 0.25−0.38 spin/$\alpha\beta$, respectively. No dependence of intensities with time was observed. The least-squares best fit to a plot of *normalized* signal intensities *vs* time yielded slope and intercept values of 0.000 min^{-1} and 1.00, respectively. The $g_{av} = 1.94$ signal intensities of the same samples varied from 0.35−0.52 spin/$\alpha\beta$, 0.50−0.61 spin/$\alpha\beta$, 0.50−0.90 spin/$\alpha\beta$, and 0.64−0.82 spin/$\alpha\beta$, respectively. In this case, there appeared to be a slight increase in spin intensities with time. The corresponding fit to the data yielded 0.001 min^{-1} slope and 0.96 intercept values.

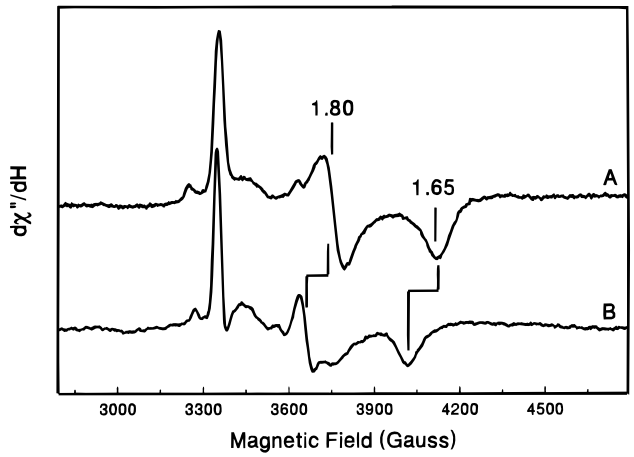

FIGURE 3: Effect of CO_2 on the $g_{av} = 1.82$ signal. (A) $CODH_{Ct}$ (32 μM $\alpha\beta$, batch 1), oxidized with thionin (7.8 equiv/$\alpha\beta$), cooled to 1 °C, and frozen 5 min later. (B) $CODH_{Ct}$ (36 μM $\alpha\beta$, batch 1) oxidized with thionin (6.6 equiv/$\alpha\beta$), exposed to 1 atm CO_2 for 3 min, then cooled to 2 °C, oxidized further (0.7 equiv/$\alpha\beta$ thionin), and then frozen 5 min later.

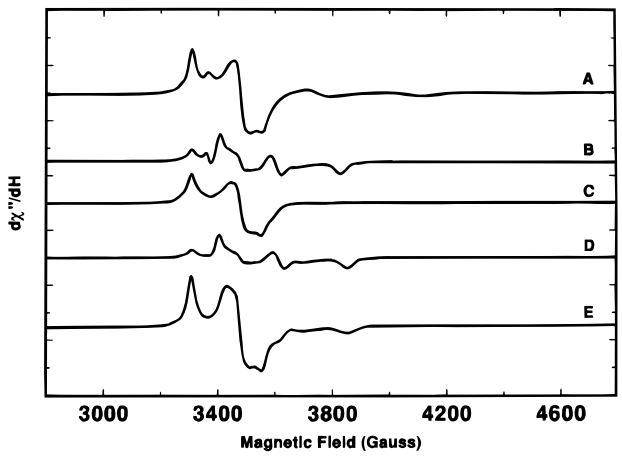

FIGURE 4: Effect of dithionite (A), CO_2/dithionite (B), and CS_2/dithionite (C) on the C_{red1}/C_{red2} conversion rate, and of CO_2 (D) and CO (E) on CS_2/dithionite-treated $CODH_{ct}$. (A) $CODH_{Ct}$ (31 μM $\alpha\beta$, batch 1), cooled to 1 °C, oxidized with thionin (4.8 equiv/$\alpha\beta$), reduced 5 min later with dithionite (64 equiv/$\alpha\beta$), and frozen 1 min later. (B) Dithionite (116 equiv/$\alpha\beta$) was added to an EPR tube chilled to 1 °C and filled with 1 atm CO_2. $CODH_{Ct}$ (32 μM $\alpha\beta$, batch 1) exposed to CO, freed of CO 15 min later, oxidized with thionin (8.2 equiv/$\alpha\beta$), exposed to 1 atm CO_2, cooled to 1 °C, oxidized further with thionin (0.7 equiv/$\alpha\beta$), injected into the EPR tube, and frozen 1.0 min later. (C) $CODH_{Ct}$ (32 μM $\alpha\beta$, batch 1) exposed to CO, freed of CO, oxidized with thionin (16 equiv/$\alpha\beta$), chilled to 1 °C, further oxidized (4 equiv/$\alpha\beta$), reacted with CS_2 (41 mM final concentration) for 5 min, reduced with dithionite (65 equiv/$\alpha\beta$), and frozen 1.2 min later. (D) $CODH_{Ct}$ (35 μM $\alpha\beta$, batch 2) oxidized with thionin (2.7 equiv/$\alpha\beta$; 5 min), reduced with dithionite (51 equiv/$\alpha\beta$; 10 min), reacted with CS_2 (8.2 mM final concentration; 2 min), analyzed by EPR and shown to have a spectrum similar to (C), and then exposed to CO_2 for 30 min. (E) As in (D) but instead of exposure to CO_2 the sample was concentrated (Centricon 100), diluted in 50 mM Tris, pH 8, reconcentrated, exposed to CO for 5 min, and then frozen.

enzyme at this potential, at a C-cluster-sensitive site. Given the reduction potentials of the C_{ox}/C_{red1} and B_{ox}/B_{red} couples, these samples appear to be poised at about −0.3 V. Since this is about 0.2 V more positive than $E^{\circ\prime}$ for CO/CO_2 (−0.52 V at pH 7), this binding of CO_2 does not appear to be a direct step in its catalytic reduction.

Effect of CO_2 on the Rate of C_{red1}/C_{red2} Conversion. CO_2 dramatically increased the rate of the C_{red1}/C_{red2} conversion by dithionite. A sample of CO_2-incubated $CODH_{Ct}$, frozen immediately after adding dithionite, exhibited the C_{red2} form of the C-cluster (Figure 4B).[5] Under approximately the same conditions, a sample lacking CO_2 exhibited the C_{red1} form (Figure 4A). Our manual mixing and slow freezing methods precluded us from determining the C_{red1}/C_{red2} conversion rate in CO_2, but we estimate that the presence of CO_2 increased this rate by *at least* a factor of 10^2. Aqueous solutions become more acidic in CO_2 (found to be ∼pH 6.3 in our solutions), and we considered that the increased rate was actually due to pH changes accompanying exposure to CO_2. However, a control sample reduced under similar conditions but in the absence of CO_2 and buffered at pH 6.3 (50 mM MES) did not undergo the C_{red1}/C_{red2} conversion as fast as the sample exposed to CO_2, indicating that CO_2, not protons, interacts with the enzyme to accelerate the conversion rate.

Batch-Dependent Ability To Convert C_{red1} to C_{red2}, and Treatment for Disabled Batches. Lindahl et al. (1990a) noticed that C-clusters in some batches of $CODH_{Ct}$ were unable to convert to the C_{red2} form upon addition of reduced viologens or dithionite. A sample of such a batch, incubated 137 min in 9.4 mM dithionite, is shown in Figure 5A. We have noticed that, when the reductant was CO, *every* batch tested converted to the C_{red2} form (Figure 5B). Moreover, when such CO-treated samples were subsequently freed of CO, oxidized with thionin (to remove residual CO) (Figure 5C), and then reduced with dithionite, they converted fully to the C_{red2} form (Figure 5D). EPR spectra obtained at low microwave power were devoid of the NiFeC signal, demonstrating the absence of residual CO in such solutions. A similar effect was observed using CO_2 and dithionite (Figure 5E). Thus, treatment with CO or CO_2/dithionite "cures" this disability. These studies suggest that the enzyme has two conformations, one that is *Able* to convert to C_{red2} with

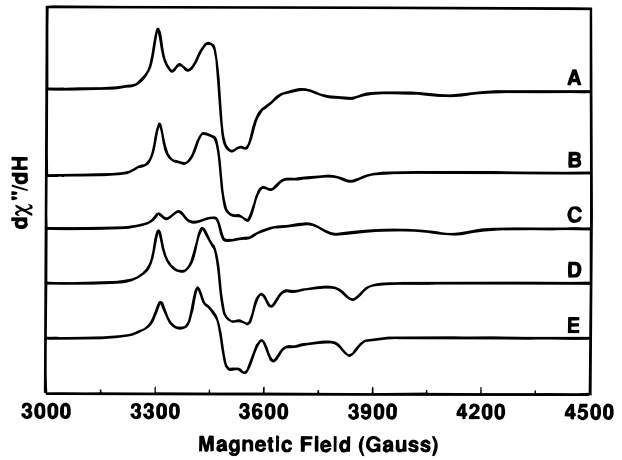

FIGURE 5: The effect of CO on C_{red1}/C_{red2}-conversion-disabled $CODH_{Ct}$. (A) $CODH_{Ct}$ (38 μM $\alpha\beta$, batch 1, 2 °C) oxidized with thionin (4.6 equiv/$\alpha\beta$), reduced 5 min later with dithionite (10 mM final concentration), and frozen after 137 min. (B) $CODH_{Ct}$ (38 μM $\alpha\beta$, batch 1, ∼28 °C) was exposed to CO, and an aliquot was transferred to an EPR tube and frozen. (C) The remainder of (B) was freed of CO by Ar degassing for 1 h, and then oxidized by thionin (2.6 equiv/$\alpha\beta$), and an aliquot was frozen after 5 min. (D) Dithionite (26 equiv/$\alpha\beta$) was added to the remainder of (C), and an aliquot was frozen after 5 min. (E) $CODH_{Ct}$ (38 μM $\alpha\beta$, batch 1, ∼28 °C) was reduced with dithionite (52 equiv/$\alpha\beta$), exposed to CO_2, and then frozen.

[5] The $g_{av} = 1.94$ signal intensity is unusually low in Figure 4B because it is saturating under these conditions (Russell and Lindahl, unpublished).

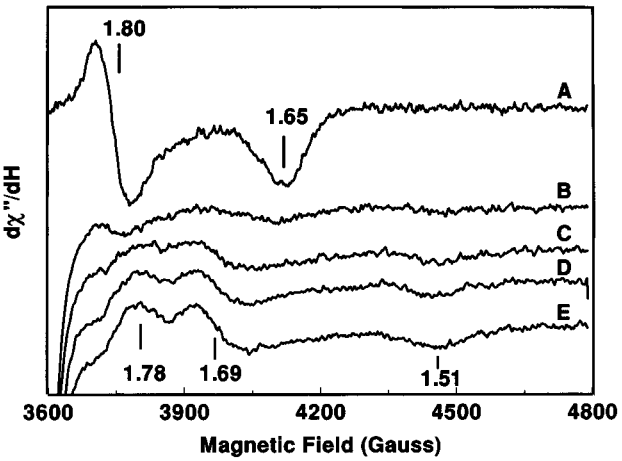

FIGURE 6: Kinetics of the CS_2/dithionite-induced C_{red1} conversion at 1 °C. (A) $CODH_{Ct}$ (32 μM $\alpha\beta$) cooled to 2 °C, oxidized with thionin (4 equiv/$\alpha\beta$), reacted with CS_2 (41 mM final concentration), and then frozen after 5 min. (B) As in (A) except reduced with dithionite (63 equiv/$\alpha\beta$) and frozen after 1.2 min. (C) As in (B) except frozen after 16 min. (D) As in (B) except frozen after 31 min. (E) As in (B) except frozen after 46 min.

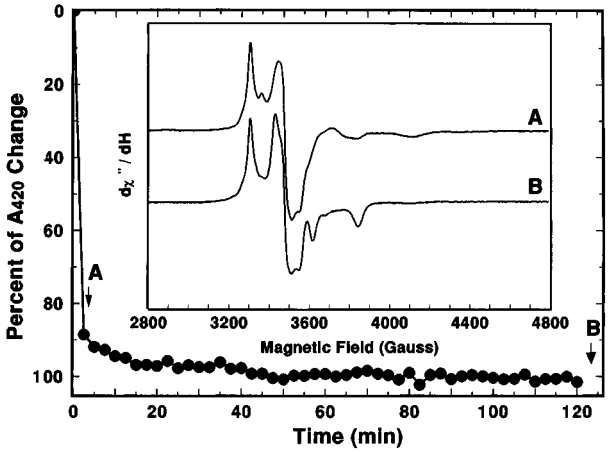

FIGURE 7: C_{red1}-to-C_{red2} conversion monitored at 420 nm and by EPR. $CODH_{Ct}$ (35 μM $\alpha\beta$, batch 1) was placed into the cuvette described in Experimental Procedures, cooled to 10 °C, oxidized with thionin (1.6 equiv/$\alpha\beta$), and monitored at 420 nm. Dithionite was added (0.9 mM final concentration), and an aliquot was withdrawn 2 min later and frozen immediately in a chilled isopentane bath. (arrow A, spectrum A). The absorbance was monitored every 2 min (circles), and a second sample was withdrawn after 125 min (arrow B, spectrum B).

dithionite, the other that is *Disabled*, and that CO_2/dithionite convert Disabled $CODH_{Ct}$ into Able $CODH_{Ct}$.

The Effect of CS_2. Carbonyl disulfide increased the rate at which dithionite effected the decay of C_{red1}. As shown in Figure 4C, C_{red1} disappeared within 1 min of adding dithionite in the presence of CS_2. However, in contrast to the effect of CO_2, the $g_{av} = 1.86$ signal did not develop. Rather, no signal initially developed as the $g_{av} = 1.82$ signal declined (Figure 6A → 6B). Slowly, an anisotropic EPR signal, apparently with $g = 1.78, 1.69, 1.51$, appeared (Figure 6C−E). The EPR-silent state of the C-cluster does not appear to reflect damaged C-clusters, since samples in this state afforded strong $g_{av} = 1.86$ signals when they were subsequently exposed to CO or CO_2 (compare Figure 4C to 4D and 4E). Finally, unlike CO_2, CS_2 did not shift the C_{red1} signal of partially-oxidized $CODH_{Ct}$ (Figure 6A).

Spectroscopic Differences between C_{red1} and C_{red2}. Evaluating the differences between C_{red1} and C_{red2} is difficult because the C-cluster cannot be prepared in isolation of the other clusters in the enzyme. However, we now have the means of examining spectroscopic differences between these two forms. This is because dithionite reduces the various clusters in $CODH_{Ct}$ at different rates. Dithionite very rapidly reduces B_{ox}, slowly converts C_{red1} into C_{red2}, and does not reduce A_{ox}. Thus, any changes in the electronic absorption spectra of $CODH_{Ct}$ ~1 min after adding dithionite probably reflect the C_{red1}/C_{red2} conversion.

A sample of thionin-oxidized $CODH_{Ct}$ was chilled to 10 °C, reduced with 1.2 mM dithionite, and monitored at 420 nm. At this wavelength, the redox state of $[Fe_4S_4]^{2+/1+}$ clusters can be monitored (the extinction coefficient of such clusters at this wavelength declines ~50% upon reduction; Shin et al., 1992). Aliquots were removed for EPR analysis after 2 and 125 min. The sample frozen 2 min after adding dithionite exhibited the $g_{av} = 1.82$ (0.21 spin/$\alpha\beta$) and 1.94 signals (0.64 spin/$\alpha\beta$) (Figure 7A), while that frozen after 125 min exhibited the $g_{av} = 1.86$ (0.24 spin/$\alpha\beta$) and 1.94 (0.58 spin/$\alpha\beta$) signals. This analysis demonstrates that the B-cluster was fully reduced and the C-cluster was in the C_{red1} state less than 2 min after adding dithionite, and that the C-cluster was fully converted to C_{red2} 125 min after adding dithionite. Approximately 90% of the total spectral changes at 420 nm occurred within the first 2 min and are associated with the reduction of B_{ox} and other species. The remaining 10% of the absorption changes occurred between 2 and 125 min, and they may be associated with the C_{red1}/C_{red2} conversion. In support of this, the rate at which this 10% change occurred is about that expected for the C_{red1}/C_{red2} conversion at 10 °C. We cannot exclude the possibility that the spectral changes arose from an unrelated reduction that occurred coincidentally with the C_{red1}/C_{red2} conversion. Assuming that each $\alpha_2\beta_2$ tetramer contains six Fe_4S_4 clusters and that the reduction of each cluster contributes equally to the spectral changes, the C_{red1}-to-C_{red2} conversion may be associated with the reduction of ~0.6 clusters per tetramer. The $g_{av} = 1.94$ and [1.82 + 1.86] EPR signal intensities for the two samples were essentially the same, suggesting that the B-clusters and C-clusters were not the species being reduced. Since dithionite does not reduce A_{ox} under these conditions (Lindahl et al., 1990b), we are uncertain which cluster was reduced. One possibility is that no Fe_4S_4 clusters were reduced during this period, but that C_{red2} absorbs less intensely at 420 nm than C_{red1}.

DISCUSSION

Further Evidence, and an Expanded Role for a Modulator Site in $CODH_{Ct}$. Two processes of $CODH_{Ct}$, namely dissociation of CN^- and reduction of A_{ox}, were previously shown to exhibit a similar reactivity pattern to dithionite, CO, CO_2, and CS_2 (Anderson & Lindahl, 1994). Neither process occurs with dithionite or low-potential viologens alone (i.e., dithionite does not cause CN^- to dissociate from the C-cluster and it cannot reduce A_{ox}), while both processes occur in the presence of CO, CO_2/dithionite, or CS_2/dithionite. Anderson and Lindahl argued (as summarized in the Introduction) that CO, CO_2, or CS_2 bound to a site on the enzyme (called the modulator) other than the site where CN^- bound.

In this paper, we provide evidence that the conversion of C_{red1} to C_{red2} exhibits a similar reactivity pattern to dithionite, CO, CO_2, and (to some extent, see below for details) CS_2. Specifically, in the presence of CO or CO_2/dithionite, this

conversion occurs very rapidly, while in the presence of dithionite alone, it occurs quite slowly. A similar reactivity pattern was observed for CN^- dissociation and A_{ox} reduction, suggesting that the C_{red1}-to-C_{red2} conversion rate is controlled by modulator binding.

We also report that CO and CO_2/dithionite (but not dithionite itself) are able to "cure" batches of $CODH_{Ct}$ that would otherwise be unable to convert C_{red1} to C_{red2}. This study suggests that the enzyme has two conformations: one that is *Able* to convert to C_{red2} with dithionite, the other that is *Disabled*. The reactivity pattern observed here (where CO and CO_2/dithionite cause a phenomenon inaccessible to dithionite alone) again suggests that modulator binding is involved; namely, that CO and CO_2 bind at the modulator and cause a conformational change that converts Disabled $CODH_{Ct}$ into Able $CODH_{Ct}$.

To summarize, our results suggest that modulator binding controls: (a) the dissociation of CN^- from the C-cluster; (b) the reduction of A_{ox}; and (c) the rate at which C_{red1} converts to C_{red2}. Modulator binding also (d) transforms enzyme in the Disabled conformation into one that is Able to be converted from C_{red1} to C_{red2}. In general, the modulator appears to alter electron-transfer properties of the clusters in the enzyme, probably via a protein conformational change, and it seems to have a close relationship to the C-cluster. Modulator binding appears to open electron pathways from dithionite (or from the B-cluster) to A_{ox} and to the site responsible for the C_{red1}/C_{red2} conversion (assumed here to be C_{red1} itself), and it may accelerate the loss of CN^- from the C-cluster. Modulator binding may also be affecting the redox potentials of sites in the enzyme. The $g_{av} = 1.86$ signal developed at more moderate potentials in the presence of CO_2 than in its absence (Lindahl et al., 1990a).

The Effect of CS_2. Previously, we found that CN^- dissociated from the C-cluster in the presence of CS_2/dithionite, and this led to the proposal that CS_2 was also binding at the modulator (Anderson & Lindahl, 1994). The dissociation process was similar to those observed with CO or CO_2/dithionite, but the rate was slower. We now report that CS_2/dithionite effects some of the other phenomena attributed to modulator binding, but that there are differences vis-à-vis CO and CO_2/dithionite. Kumar et al. (1994) reported that CS_2 was a weak noncompetitive inhibitor of CO oxidation and CO_2 reduction, that it was a mixed inhibitor of CO/acetyl-CoA exchange activity, and that it interacted with the A-cluster and afforded an EPR signal from that cluster with $g_{av} = 2.15$ ($g = 2.2, 2.087, 2.017$). We have observed this signal, and agree with their conclusion that CS_2 interacts at the A-cluster. However, Kumar et al. (1994) reported (without showing supporting spectra or data) that CS_2 "does not change the morphologies, intensities, or relaxation properties" of the C-cluster's EPR signals, and concluded that CS_2 inhibited CO oxidation/CO_2 reduction *exclusively* through its interaction at the A-cluster. Our results indicate that CS_2 in the presence of dithionite alters the C-cluster's EPR signals (it accelerates the loss of the $g_{av} = 1.82$ signal, prevents development of the $g_{av} = 1.86$ signal, and causes the slow development of a new C-cluster signal with $g = 1.78, 1.69, 1.51$). This is evidence that CS_2 binds at or near the C-cluster.

Ensign (1995) recently reported that CS_2 is a *competitive* inhibitor of the CO_2 reduction reaction of the CODH from *Rhodospirillium rubrum* ($CODH_{Rr}$) and concluded that CS_2 mimicked CO_2 as a ligand at the active site. It is surprising that CS_2 would be a noncompetitive inhibitor of CO oxidation/CO_2 reduction for $CODH_{Ct}$, yet a competitive inhibitor for $CODH_{Rr}$, since the two enzymes are so similar. The amino acid sequences of $CODH_{Rr}$ and the β subunit of $CODH_{Ct}$ are 46% identical (Kerby et al., 1992), both enzymes contain virtually identical C- and B-clusters (Hu et al., 1996), and both CN^--inhibited enzymes are reactivated by CO, CO_2/dithionite, and CS_2/dithionite (Ensign et al., 1989; Hyman et al., 1989; Anderson & Lindahl, 1994). These similarities, our evidence that CS_2 binding affects the C-cluster, and the isoelectronic and isostructural nature of CO_2 and CS_2 all suggest that CS_2 competes with CO_2 for the same site. On the other hand, the results of Kumar et al. (1994), and the somewhat different behavior of CO_2 and CS_2 toward $CODH_{Ct}$ observed here, suggest that the CS_2 binding properties of $CODH_{Ct}$ and $CODH_{Rr}$ are not identical. Further experiments appear to be required to clarify whether CS_2 is a noncompetitive or competitive inhibitor of CO_2 reduction in $CODH_{Ct}$.

The Identity of the Modulator. We assumed the existence of a modulator site to explain the effects of CO, CO_2/dithionite, and CS_2/dithionite. These effects required that the modulator be *electronically isolated* from the C-cluster and be redox active (CO_2 and CS_2 bind to the reduced state, CO binds to the oxidized state). The requirement that the modulator be electronically isolated from the C-cluster allowed us to rationalize how CO could prevent CN^- from binding the C_{red2} state of the C-cluster without binding C_{red2} itself (we did not want to propose that CO bound C_{red2}, since nonligating reductants like dithionite and viologens to $CODH_{Ct}$ can also yield the C_{red2} state). The modulator was thought to be redox active because CO_2 and CS_2 were unable to accelerate the dissociation of CN^- in the absence of a reductant. However, in spite of being electronically isolated from the C-cluster, the modulator was thought to be closely associated with the C-cluster (since binding the modulator accelerates the dissociation of CN^- and, as we have shown here, the C_{red1}/C_{red2} conversion rate).

Hu et al. (1996) recently used Mössbauer spectroscopy to determine that the C-cluster consists of an $[Fe_4S_4]^{2+/1+}$ cluster linked to a Ni center. One of the irons in the cube appears to be 5-coordinate (called FCII), and this is probably the iron that bridges the cluster to the Ni. CN^- was found to bind to FCII. In the C_{red1} state, the Fe_4S_4 cluster has a 1+ core oxidation state and the Ni center is almost certainly Ni^{2+}. Surprisingly, the $g_{av} = 1.82$ signal appears to arise predominately (or exclusively) from the $[Fe_4S_4]^{1+}$ cluster portion of the C-cluster; the Ni center appears to be either weakly coupled to the cube or not coupled at all. This conclusion is based on the fact that the $g_{av} = 1.82$ signal is not hyperfine-broadened by ^{61}Ni and that the $g_{av} = 1.82$ electronic state is quite similar to the $[Fe_4S_4]^{1+}$ cluster in the Ni-free enzyme aconitase, with citrate bound to one of the irons of the cube ($g = 2.01, 1.875, 1.796$; Telser et al., 1986). Alternatively, the Ni could be high-spin Ni^{2+} ($S = 1$) and this could spin-couple weakly with the cluster. A coupling model derived using these assumptions (Hu et al., 1996) can explain the unusual EPR signal ($g > 2.0$) obtained from the C-cluster in the presence of SCN^- or N_3^- (Seravalli et al., 1995).

In light of these developments, we now propose that the Ni ion of the C-cluster is the modulator. Because the Ni is either weakly coupled, or not coupled at all to the $[Fe_4S_4]^{1+}$ cluster yielding the $g_{av} = 1.82$ and 1.86 signals, CO, CO_2,

and CS_2 may bind to the Ni without affecting the electronic state of the cluster. Because of the close proximity of the Ni to the Fe_4S_4 cluster, steric and/or electronic effects may be responsible for accelerating the dissociation of CN^- from FCII and altering the C_{red1}/C_{red2} conversion rate.

The model also allows us to rationalize the behavior of CO, CO_2, and CS_2. Since CO does not shift the C_{red2} signal, it may bind exclusively to the Ni in this form. Since CO_2 shifts the C_{red1} signal, it may bind to both the Ni and an Fe of the cube. Since CO_2 has no effect on C_{red2}, it may bind only to the Ni in this state. Since CS_2 does not shift the C_{red1} signal, it might bind exclusively to the Ni moiety in the C_{red1} form. But since CS_2 shifts the C_{red2} signal to one with $g_{av} = 1.66$ in the reduced enzyme, it may bind the Ni and an Fe in this state. Other inhibitors like N_3^-, OCN^-, and SCN^- appear to have a dramatic effect on the coupling of the C-cluster, probably because they bridge the Ni and an Fe of the cube (Seravalli et al., 1995).

Direct spectroscopic evidence for the modulator is needed to establish its existence. The effect of CO_2 on the $g_{av} = 1.82$ EPR signal establishes that CO_2 can bind to a C-cluster-sensitive site at mild potentials. This CO_2 binding site may be the modulator, but this is not known with certainty. If it is the modulator, CN^- would appear to dissociate by a mechanism somewhat different than we proposed earlier (Anderson & Lindahl, 1994). We proposed that CN^- dissociation was caused by the binding of CO, CO_2, and CS_2 to the modulator, that the modulator was redox active, and that CO_2 and CS_2 could only bind to its reduced state. Our present results indicate that CO_2 binds to a site on the enzyme when the C-cluster is in the C_{red1} state. However, our previous results indicate that CO_2 cannot accelerate the dissociation of CN^- when the enzyme is poised in this state (see Figure 6 of Anderson & Lindahl, 1994; diamonds). The enzyme must be further reduced before CN^- dissociates. Thus, CN^- dissociation appears to involve not only modulator binding but a reduction event as well. We will argue below that this reduction corresponds to the C_{red1}/C_{red2} conversion.

Mechanism for CO Oxidation and CO_2 Reduction. One of our long-term goals is to understand the mechanism of catalysis in CODHs. The results presented here, and the following properties of the enzyme, severely restrict the possible mechanisms. First, only one active-site cluster (the C-cluster) and one $n = 1$ electron-transfer cluster (the B-cluster) are required for catalysis (Hu et al., 1996). The $[Fe_4S_4]^{2+/1+}$ B-cluster transfers electrons, *one at a time*, between the C-cluster and external electron acceptors such as methyl viologen (MV^{2+}/MV^{1+}). Second, catalysis appears to proceed by a ping-pong mechanism, in which CO binds to the C-cluster, delivers two electrons to it, and departs in the form of CO_2 before methyl viologen is reduced (Seravalli et al., 1995). This indicates that the two-electron-reduced form of the enzyme is stable. Third, the ability of the enzyme to operate in reverse suggests that CO_2 binds to a stable two-electron-reduced form of the C-cluster, extracts two electrons from it, deposits an OH^- on the enzyme, and leaves in the form of CO. Fourth, since low-potential electron acceptors such as MV^{2+} can be used in catalysis, catalytically-relevant states of the C- and B-clusters should be stable within ~0.1 V of $E^{\circ\prime}$s for the CO/CO_2 couple (−0.52 V) and the MV^{2+}/MV^{1+} couple (−0.44 V), i.e., between about −0.3 and −0.6 V. This effectively excludes the C_{ox} state from participating in catalysis, because it is present at potentials outside of these limits ($E^{\circ\prime}$ for $C_{ox}/C_{red1} = -220$ mV).

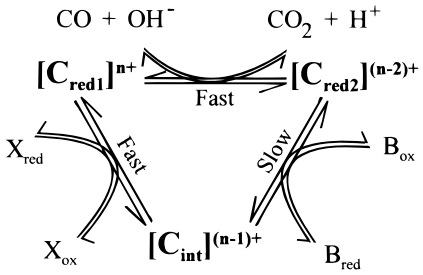

FIGURE 8: Model of CO oxidation/CO_2 reduction catalysis by CODHs.

These properties would seem to require that, during catalysis, the C-cluster traverses three sequential oxidation states, labeled C^{n+}, $C^{(n-1)+}$, and $C^{(n-2)+}$, and that these states react with CO, CO_2, the B-cluster, and an unidentified species X, as shown in Figure 8. We previously proposed that C_{red1} ($S = {}^1/_2$) and C_{red2} ($S = {}^1/_2$) were the C^{n+} and $C^{(n-2)+}$ states, respectively (Anderson & Lindahl, 1994), and this forms the basis of our model. In this model, $[C_{red1}]^{n+}$ binds CO, is reduced by two electrons to $[C_{red2}]^{(n-2)+}$, and releases CO_2. $[C_{red2}]^{(n-2)+}$ reduces B_{ox}, affording the state $[C_{int}]^{(n-1)+}$. $[C_{int}]^{(n-1)+}$ reduces X_{ox}, returning to the state $[C_{red1}]^{n+}$. B_{red} and X_{red} are reoxidized by external redox agents such as methyl viologen.

We have introduced species X to make this model compatible with all published results relevant to CO/CO_2 redox catalysis. For example, CO reduction of enzyme in the C_{red1} state and with the B-cluster oxidized affords the C_{red2} and B_{red} states (i.e., fully reduced enzyme exhibits the $g_{av} = 1.94$ and 1.86 EPR signals). If X was not included, two-electron reduction of C_{red1} by CO would yield C_{red2}, and a subsequent one-electron reduction of B_{ox} by C_{red2} would yield B_{red} and C_{int}. Given that C_{int} cannot be reduced by a second CO (this state can only accept one electron, and CO is a two-electron donor), a model that does not include X predicts that fully-reduced enzyme would exhibit only the $g_{av} = 1.94$ signal. By introducing X, C_{int} can reduce X_{ox}, and a second molecule of CO can reduce the resulting C_{red1} state to C_{red2}. Accordingly, fully-reduced enzyme would exhibit the $g_{av} = 1.86$ and 1.94 signals, as observed.

Species X must also be introduced to explain the results of Kumar et al. (1993). They reacted partially-oxidized CODH in the C_{red1} state with CO and monitored the pre-steady-state changes by EPR. The first event to occur was the decline of the $g_{av} = 1.82$ signal and the development of the $g_{av} = 1.86$ signal. This was followed by the slow development of the $g_{av} = 1.94$ signal as the $g_{av} = 1.86$ signal intensity remained constant. This behavior is explained by our model as follows. CO rapidly binds and reduces C_{red1} to C_{red2}, and then C_{red2} slowly reduces B_{ox}, forming C_{int} and B_{red}. Without species X, the model would predict that the $g_{av} = 1.86$ should *decay* as the $g_{av} = 1.94$ signal develops. By including X, C_{int} could rapidly reduce X_{ox}, re-forming C_{red1}, and a second molecule of CO could rapidly reduce C_{red1}, forming C_{red2}. Since these last two steps would be rapid, the C_{int} state would not be observed, and the C_{red2} state would appear constant as the $g_{av} = 1.94$ signal developed.

The identity of species X is uncertain, and it is not necessarily another cluster in CODH. For example, CODH molecules may be able to undergo intermolecular electron transfer, and X may actually be another CODH molecule.

We have also considered that a major assumption of our model (that C_{red2} is two electrons more reduced than C_{red1}) is incorrect, and that X is an artifact of this incorrect assumption. We have formulated a model in which C_{red1} and C_{red2} are assumed to be isoelectronic, but this model is more complicated and unrealistic than the one we favor.[6] Thus we regard this possibility as unlikely.

Comparison to Other CO/CO_2 Ni Catalysts. It is edifying to compare the mechanism of CO/CO_2 redox proposed for CODH to those proposed for well-characterized Ni complexes with biologically-relevant ligands that catalyze the same reaction. Lu and Crabtree (1994) report that Ni^{2+} iminothiolate complexes (e.g., $[Ni(C_{12}H_{13}N_3OS)]_2$) catalytically oxidize CO to CO_2 using methyl viologen as an electron acceptor. They proposed that CO binds to Ni^{2+} and is attacked by OH^-. After deprotonation, CO_2 loss occurs in concert with a one-electron oxidation of the Ni complex. The resulting Ni^{1+} complex is oxidized by a second methyl viologen, returning the complex to the Ni^{2+} state.

Ni(cyclam) (cyclam = 1,4,8,11-tetraazatetradecane) catalyzes the electrochemical reduction of CO_2 to CO (Beley et al., 1986). One-electron-reduced Ni^{1+} cyclam binds and reduces CO_2, affording $Ni^{3+}-CO_2^-$. After protonation, the complex is reduced rapidly to $Ni^{2+}-COOH$, thereby weakening the C−OH bond. Dissociation of OH^- and CO affords the Ni^{2+} state. Sakaki (1992) calculated the energy of simplified versions of these catalytic states (he replaced cyclam with four NH_3 ligands) using the *ab initio* MO/SD-CI method. He found that CO_2 can coordinate to the axial position of a planar $Ni(NH_3)_4$ fragment as long as the Ni is in the 1+ state and an anionic ligand (F^- was used in his calculations) is coordinated in the other axial position. The anion neutralizes the positive charge on the Ni^{1+} (thereby reducing the charge−dipole repulsion associated with the approach of a bending CO_2 to the complex) and destabilizes the filled d_{z^2} orbital (thereby enhancing the charge transfer from this orbital to the empty π^* orbital of CO_2 that is eventually used for coordination).

An important implication of these studies is that the C-cluster state that binds CO_2 (i.e., C_{red2}) probably contains Ni^{1+}. These studies also suggest that the overall charge on the complex in this state is probably small (to reduce the charge−dipole repulsion) and that an anionic ligand (cys, asp, glu) may be coordinated opposite of the CO_2 binding site.

Oxidation State Assignments of C_{red1} and C_{red2}. Hu et al. (1996) concluded that the Ni and Fe_4S_4 cluster in C_{red1} are in the 2+ and 1+ states, respectively. Assuming that C_{red2} is two electrons more reduced than C_{red1}, how might the two additional electrons be assigned? Ni can be stabilized in the 3+, 2+, and 1+ states when coordinated to biological ligands (Lancaster, 1988), and Fe_4S_4 clusters can be stabilized in the 3+, 2+, and 1+ core oxidation states. Since C_{red2} is proposed to be the form that binds CO_2, and the model studies described above indicate that CO_2 reacts with Ni^{1+} species, we assign one electron to the Ni, generating Ni^{1+}. Assigning the second electron is more difficult. An $[Fe_4S_4]^0$ cluster has been proposed (Surerus et al., 1992) for the reduced state of the nitrogenase P-clusters (a unique bridged pair of Fe_4S_4 clusters), and so it is possible that this state is present in the C_{red2} form. However, the local spin of the $[Fe_4S_4]^0$ cluster would be either $S = 0$ or integer, and coupling to a Ni^{1+} would yield an electronic state substantially different from the $g_{av} = 1.86$ state (Hu and Münck, personal communications). Since the $g_{av} = 1.82$ and 1.86 signals appear so similar, the Fe_4S_4 moiety of the C-cluster would appear to be isoelectronic (i.e., in the 1+ core state) in C_{red1} and C_{red2}. The only other option is that the Ni center accommodates the second electron. One possibility is that the Ni coordinates a redox-active ligand that is reduced and spin-coupled to the Ni^{1+} ion in the C_{red2} state. A related phenomenon occurs in galactose oxidase, where a redox-active tyrosine is coordinated and spin-coupled to Cu^{2+} (Ito et al., 1991). Thus, the oxidation state assignments that appear to be most compatible with the relevant results are $\{L_{ox}^{n+}, Ni^{2+}, [Fe_4S_4]^{2+}\}^{(m)+}$ for C_{ox}, $\{L_{ox}^{n+}, Ni^{2+}, [Fe_4S_4]^{1+}\}^{(m-1)+}$ for C_{red1}, and $\{L_{red}^{(n-1)+}, Ni^{1+}, [Fe_4S_4]^{1+}\}^{(m-3)+}$ for C_{red2}.

Conclusions. The results and conclusions of this paper can be summarized by the following model. The C_{red1} state of the C-cluster is a Ni^{2+} complex with a redox-active ligand L_{ox}, bridged to an $[Fe_4S_4]^{1+}$ cube. C_{red2} is two electrons more reduced than C_{red1}, with one electron assigned to the Ni (affording Ni^{1+}) and the other assigned to the redox-active ligand (L_{red}). Dithionite can slowly reduce the $\{L_{ox}^{n+}\ Ni^{2+}\}$ center of C_{red1} into the $\{L_{red}^{(n-1)+}\ Ni^{1+}\}$ center of C_{red2}. Both CO and CO_2 can bind the Ni center in C_{red1}. Two electrons from the bound CO are rapidly transferred to the Ni center to yield CO_2 and the C_{red2} state. CO_2 binds C_{red1} noncatalytically (i.e., without accepting an electron pair from the center) but in a manner that perturbs the $g_{av} = 1.82$ signal originating predominately from the $[Fe_4S_4]^{1+}$ portion of the C-cluster. This binding also accelerates the reduction of the Ni center by dithionite (forming C_{red2}), either by altering the reduction potential of the site or the electron-transfer kinetics from dithionite to the C-cluster. This binding also allows A_{ox} to be reduced by dithionite.

The potent inhibitor CN^- binds to the FCII iron of the $[Fe_4S_4]^{1+}$ portion of the C-cluster in the C_{red1} state. CN^- dissociates after CO binds to the Ni center and reduces the center by two electrons. CN^- also dissociates after CO_2 binds and dithionite reduces the center. Thus, k_{obs} for CN^- dissociation (Anderson & Lindahl, 1994) would correspond

[6] Consider a model in which C_{red2} is isoelectronic with C_{red1}, and call this state C_{red12}. The triangular catalytic cycle described in Figure 8 still applies, since it was constructed to explain how catalysis can occur, given the $n = 2$ nature of the CO/CO_2 reaction, the $n = 1$ nature of the B_{red}/B_{ox} couple, and evidence that the enzyme is stable in a two-electron-reduced form. Since the C_{red1}-to-C_{red2} conversion is a redox-dependent process, and no EPR signals besides those from the C-cluster appear to change during that conversion, this model requires that CODH contains an EPR-silent redox species Y, such that reduction of Y ($E^{\circ\prime} = -530$ mV) converts the $g_{av} = 1.82$ signal to the $g_{av} = 1.86$ signal. Since C_{ox} does not appear to participate in catalysis, the C_{red12} state (being one electron more reduced than C_{ox}) would be the catalytic state that reacts with CO. CO_2 presumably would react with a C-cluster state two electrons more reduced than C_{red12}, but no such state is known. This model must assume the existence of such a state, to be called $C_{superred}$. As was the case with the model described in the text (in which C_{red2} was proposed to be two electrons more reduced than C_{red1}), this model also requires a species X to render it fully compatible with the relevant results. However, the proposed $C_{superred}$ state is unrealistic, for it should be stable at potentials substantially more negative than −600 mV (the $g_{av} = 1.86$ form of C_{red12} is stable at −600 mV (Lindahl et al., 1990a), and $C_{superred}$ is proposed to be two electrons more reduced than C_{red12}). But $E^{\circ\prime}$ for CO/CO_2 is only −0.52 V (pH 7), and so CO does not seem to have enough reducing power to reduce C_{red12} to the hypothetical $C_{superred}$ state. In summary, the isoelectronic model assumes everything assumed by the model described in the text, plus it assumes another redox-active species Y (whose reduction effects the C_{red1}-to-C_{red2} conversion) and a $C_{superred}$ state that would be generated at unrealistically low potentials.

to k_{off} of CN^- from the C_{red2} state of the C-cluster. CS_2 reacts similarly to CO_2.

Catalysis requires one active-site C-cluster, one electron-transfer $[Fe_4S_4]^{2+/1+}$ B-cluster, and one unidentified $n = 1$ redox agent X. The C-cluster traverses three sequential redox states in catalysis: C_{red1}, C_{int}, and C_{red2}. During CO oxidation catalysis, CO binds and is oxidized by C_{red1}. During CO_2 reduction catalysis, CO_2 binds and is reduced by C_{red2}. C_{int} is obtained after a one-electron transfer to either the B-cluster or species X. This model requires the assumption of X, L, and the C_{int} state to render it compatible with all relevant experimental results.

Although this model for the C_{red1}-to-C_{red2} conversion, CN^- dissociation, and CO oxidation/CO_2 reduction catalysis may be ultimately superseded by superior models, it is the first and only model proposed to date that unifies and explains all the relevant properties of the enzyme. We hope it will stimulate further mechanistic studies of this highly complex metalloenzyme.

ACKNOWLEDGMENT

We thank Eckard Münck and Ed Hu for helpful discussion, Marcetta Y. Darensbourg for use of the UV−vis spectrophotometer, Donald J. Darensbourg for providing the CS_2, Jinqiang Xia for providing some of the enzyme (batch 2), and Genero Medina for help with some of the CO_2 experiments.

REFERENCES

Anderson, M. E., & Lindahl, P. A. (1994) *Biochemistry 33*, 8702−8711.
Anderson, M. E., DeRose, V. J., Hoffman, B. M., & Lindahl, P. A. (1993) *J. Am. Chem. Soc. 115*, 12204−12205.
Averill, B. A., Bale, J. R., & Orme-Johnson, W. H. (1978) *J. Am. Chem. Soc. 100*, 3034−3043.
Beley, M., Collin, J.-P., Ruppert, R., & Sauvage, J.-P. (1986) *J. Am. Chem. Soc. 108*, 7461−7467.
Ensign, S. A. (1995) *Biochemistry 34*, 5372−5381.
Ensign, S. A., Hyman, M. R., & Ludden, P. W. (1989) *Biochemistry 28*, 4973−4979.
Fan, C., Gorst, C. M., Ragsdale, S. W., & Hoffman, B. M. (1991) *Biochemistry 30*, 431−435.
Gordon, A. J., & Ford, R. A. (1971) *The Chemists Companion*, p 432, Wiley Interscience, New York.
Gorst, C. M., & Ragsdale, S. W. (1991) *J. Biol. Chem. 266*, 20687−20693.
Hu, Z., Spangler, N. J., Anderson, M. E., Xia, J., Ludden, P. W., Lindahl, P. A., & Münck, E. (1996) *J. Am. Chem. Soc., 118*, 830−845.
Hyman, M. R., Ensign, S. A., Arp, D. J., & Ludden, P. W. (1989) *Biochemistry 28*, 6821−6826.
Ito, N., Phillips, S. E. V., Stevens, C., Ogel, Z. B., McPherson, M. J., Keen, J. N., Yadav, K. D. S., & Knowles, P. F. (1991) *Nature 350*, 87−90.
Kerby, R. L., Hong, S. S., Ensign, S. A., Coppoc, L. J., Ludden, P. W., & Roberts, G. P. (1992) *J. Bacteriol. 174*, 5284−5294.
Kumar, M., & Ragsdale, S. W. (1992) *J. Am. Chem. Soc. 114*, 8713−8715.
Kumar, M., Lu, W.-P., Liu, L., & Ragsdale, S. W. (1993) *J. Am. Chem. Soc. 115*, 11646−11647.
Kumar, M., Lu, W.-P., & Ragsdale, S. W. (1994) *Biochemistry 33*, 9769−9777.
Lancaster, J. R., Ed. (1988) *The Bioinorganic Chemistry of Nickel*, VCH, New York.
Lindahl, P. A., Münck, E., & Ragsdale S. W. (1990a) *J. Biol. Chem. 265*, 3873−3879.
Lindahl, P. A., Ragsdale, S. W., & Münck, E. (1990b) *J. Biol. Chem. 265*, 3880−3888.
Lu, W.-P., & Ragsdale, S. W. (1991) *J. Biol. Chem. 266*, 3554−3564.
Lu, Z., & Crabtree, R. H. (1995) *J. Am. Chem. Soc. 117*, 3994−3998.
Lundie, L. L., Jr., & Drake, H. L. (1984) *J. Bacteriol. 159*, 700−703.
Morton, T. A., Runquist, J. A., Ragsdale, S. W., Shanmugasundaram, T., Wood, H. G., & Ljungdahl, L. G. (1991) *J. Biol. Chem. 266*, 23824−23828.
Pelley, J. W., Garner, C. W., & Little, G. H. (1978) *Anal. Biochem. 86*, 341−343.
Qiu, D., Kumar, M., Ragsdale, S. W., & Spiro, T. G. (1994) *Science 264*, 817−819.
Qiu, D., Kumar, M., Ragsdale, S. W., & Spiro, T. G. (1995) *J. Am. Chem. Soc. 117*, 2653−2654.
Ragsdale, S. W. (1991) *CRC Crit. Rev. Biochem. Mol. Biol. 26*, 261−300.
Ragsdale, S. W., Ljungdahl, L. G., & DerVartanian, D. V. (1982) *Biochem. Biophys. Res. Commun. 114*, 658−663.
Ragsdale, S. W., Clark, J. E., Ljungdahl, L. G., Lundie, L. L., & Drake, H. L. (1983) *J. Biol. Chem. 268*, 2364−2369.
Ragsdale, S. W., Wood, H. G., & Antholine, W. E. (1985) *Proc. Natl. Acad. Sci. U.S.A. 82*, 6811−6814.
Roberts, J. R., Lu, W. P., & Ragsdale, S. W. (1992) *J. Bacteriol. 174*, 4667−4676.
Sakaki, S. (1992) *J. Am. Chem. Soc. 114*, 2055−2062.
Seravalli, J., Kumar, M., Lu, W.-P., & Ragsdale, S. W. (1995) *Biochemistry 34*, 7879−7888.
Shin, W., & Lindahl, P. A. (1992a) *Biochemistry 31*, 12870−12875.
Shin, W., & Lindahl, P. A. (1992b) *J. Am. Chem. Soc. 114*, 9718−9719.
Shin, W., & Lindahl, P. A. (1993) *Biochim. Biophys. Acta 1161*, 317−322.
Shin, W., Stafford, P. R., & Lindahl, P. A. (1992) *Biochemistry 31*, 6003−6011.
Shin, W., Anderson, M. E., & Lindahl, P. A. (1993) *J. Am. Chem. Soc. 115*, 5522−5526.
Surerus, K. K., Hendrich, M. P., Christie, P. D., Rottgardt, D., Orme-Johnson, W. H., & Münck, E. (1992) *J. Am. Chem. Soc. 114*, 8579−8590.
Telser, J., Emptage, M. H., Merkle, H., Kennedy, M. C., Beinert, H., & Hoffman, B. M. (1986) *J. Biol. Chem. 262*, 4840−4846.
Weber, K., & Osborn, M. (1969) *J. Biol. Chem. 244*, 4406−4412.
Wood, H. G., & Ljungdahl, L. G. (1990) in *Variations in Autotropic Life* (Shively, J. M., & Barton, L. L., Eds.) pp 201−250, Academic Press, London, 1991.
Xia, J., & Lindahl, P. A. (1995) *Biochemistry 34*, 6037−6042.
Xia, J., & Lindahl, P. A. (1996) *J. Am. Chem. Soc. 118*, 483−484.
Xia, J., Dong, J., Wang, S., Scott, R. A., & Lindahl, P. A. (1995) *J. Am. Chem. Soc. 117*, 7065−7070.
Xia, J., Sinclair, J. F., Baldwin, T. O., & Lindahl, P. A. (1996) *Biochemistry 35*, 1965−1971.

BI952902W